9950-965

DOE/JPL 955533-83/08
Distribution Category UC-63

DEVELOPMENT OF A POLYSILICON PROCESS BASED ON CHEMICAL VAPOR DEPOSITION OF DICHLOROSILANE IN AN ADVANCED SIEMEN'S REACTOR

Contract 955533

Modification No. 15

Final Report

Covering the Period

October 11, 1982 to May 21, 1983

Dr. James R. McCormick, Program Manager
Arvid N. Arvidson, Principal Investigator
David H. Sawyer
David M. Muller

Hemlock Semiconductor Corporation
12334 Geddes Road
Hemlock, Michigan 48626

July 14, 1983

"The JPL Flat-Plate Solar Array Project is sponsored by the U. S. Department of Energy and forms part of the Solar Photovoltaic Conversion Program to initiate a major effort toward the development of low-cost solar arrays. This work was performed for the Jet Propulsion Laboratory, California Institute of Technology by agreement between NASA and DOE."

DOE/JPL 955533-83
Distribution Category UC-63

DEVELOPMENT OF A POLYSILICON PROCESS BASED ON CHEMICAL VAPOR DEPOSITION OF DICHLOROSILANE IN AN ADVANCED SIEMEN'S REACTOR

Contract 955533

Modification No. 15

Final Report

Covering the Period

October 11, 1982 to May 21, 1983

Dr. James R. McCormick, Program Manager
Arvid N. Arvidson, Principal Investigator
David H. Sawyer
David M. Muller

Hemlock Semiconductor Corporation
12334 Geddes Road
Hemlock, Michigan 48626

July 14, 1983

"The JPL Flat-Plate Solar Array Project is sponsored by the U. S. Department of Energy and forms part of the Solar Photovoltaic Conversion Program to initiate a major effort toward the development of low-cost solar arrays. This work was performed for the Jet Propulsion Laboratory, California Institute of Technology by agreement between NASA and DOE."

HSC HEMLOCK SEMICONDUCTOR CORPORATION
a wholly owned subsidiary of Dow Corning Corporation
12334 Geddes Rd., Hemlock, Michigan 48626

ABSTRACT

Dichlorosilane (DCS) was used as the feedstock for an advanced decomposition reactor for silicon production. The advanced reactor had a cool bell jar wall temperature, 300°C, when compared to Siemen's reactors previously used for DCS decomposition by Hemlock Semiconductor Corporation. Previous reactors had bell jar wall temperatures of approximately 750°C.

The cooler wall temperature allows higher DCS flow rates and concentrations. A silicon deposition rate of 2.28 gm/hr-cm was achieved with power consumption of 59 kWh/kg. Interpretation of data suggests that a 2.8 gm/hr-cm deposition rate is possible. The 2.8 gm/hr-cm deposition rate surpasses the goal of 2.0 gm/hr-cm. Power consumption and conversion should approach the program goals of 60 kWh/kg and 40%.

Screening of lower cost materials of construction was done as a separate program segment. Stainless Steel (304 and 316), Hastalloy B, Monel 400 and 1010-1020 Carbon Steel were placed individually in an experimental scale reactor. Silicon was deposited from trichlorosilane feedstock. The resultant silicon was analyzed for electrically active and metallic impurities as well as carbon. No material contributed significant amounts of electrically active or metallic impurities, but all contributed carbon. Single crystal growth could not be maintained in most zone refining evaluations. No material need be excluded from consideration for use in construction of decomposition reactor components for production of photovoltaic grade silicon; however, further evaluation and the use of the low carbon alloys is considered essential.

TABLE OF CONTENTS

LIST OF TABLES

LIST OF FIGURES

1.0 Summary

This report describes experimentation and provides discussion of results for the chemical vapor deposition of silicon from dichlorosilane (DCS) in an advanced decomposition reactor.

Specific tasks accomplished during this program are summarized as follows:

Existing equipment and procedures were modified to allow safe decomposition of DCS in an advanced reactor at Hemlock Semiconductor Corporation.

Twenty DCS decomposition runs were made using various DCS feed rates and concentrations. Other variables investigated were feed nozzle velocity and rod temperature.

Silicon produced was evaluated for electrically active contaminants and carbon. Three runs were evaluated for metallic impurities by spark source mass spectroscopy.

Gas chromatographic analysis was performed on vent gases from the reactor to determine mass balance.

Materials of construction alternatives were evaluated.

A theoretical evaluation was made to determine the impact of jar emissivity on power consumption.

A key result of this program was the high deposition rate and low power consumption achieved.

Higher DCS flow rates and concentrations were utilized in the advanced reactor. A silicon deposition rate of 2.28 gm/hr-cm was achieved with power consumption of 59 kWh/kg. Interpretation of data suggests that a 2.8 gm/hr-cm deposition

rate is possible. The 2.8 gm/hr-cm deposition rate surpasses the goal of 2.0 gm/hr-cm. Power consumption and conversion should simultaneously approach the program goals of 60 kWh/kg and 40%.

Reactor materials of construction were evaluated in a separate reactor system. No potential reactor material of construction contributed significant amounts of electrically active or metallic impurities, but all materials contributed carbon. Single-crystal growth could not be maintained in most zone refining evaluations of this material. No material need be excluded from consideration for use in construction of decomposition reactor components for the production of photovoltaic-grade silicon; however, further evaluation and the use of the low-carbon alloys is considered essential.

2.0 Introduction

2.1 Objective

Hemlock Semiconductor Corporation (HSC) previously investigated and reported results of the production of polycrystalline silicon from the decomposition of dichlorosilane.[1] While performance of reactors using dichlorosilane feed was significantly better than reactors using trichlorosilane, the performance was less than desired. Deposition of silicon on the bell jar limited feed rates and concentrations of dichlorosilane to the reactor. Consequently, deposition rates, power consumption and conversion efficiency goals were not simultaneously met.

The objective of this effort was to attain deposition rate and power consumption goals of:

Deposition Rate	2.0 gm/hr-cm
Power Consumption	60 kWh/kg
Conversion Efficiency	40%

Demonstration of these goals would allow a more accurate assessment of dichlorosilane's potential as a feedstock

for the production of polycrystalline silicon.

In addition, materials of construction were evaluated in an effort to identify lower-cost alternatives for reactor materials of construction.

2.2 Approach

Dichlorosilane (DCS) was fed to a cooled-wall decomposition reactor. Various feed rates and concentrations, as well as rod temperature and feed nozzle velocity, were tested in a scan of conditions directed at achieving the deposition rate and power consumption goals. Results were obtained for deposition rate, conversion efficiency, power consumption, and jar deposition. Gas chromatographic analysis of the feed and vent streams from several reactor runs provided mass balance information.

Materials of construction were tested by placing a cleaned coil of tubing of the material to be evaluated inside an experimental scale reactor, and producing silicon by decomposition of trichlorosilane. The resultant silicon was evaluated for electrically active contaminants, carbon, and metals.

3.0 Technical Progress

3.1 Design and Installation of Feed DCS on an Advanced Reactor

Necessary equipment and procedural modifications were made to allow dichlorosilane to be safely fed to an existing cooled-wall reactor at HSC. This air-cooled deposition reactor is configured the same as the Model 8D reactor used in HSC's previous program.[1] Modification to liquid cooling, while anticipated, would have caused program delay. Air cooling was found to be adequate to achieve reactor performance objectives.

3.2 Advanced Reactor Performance

3.2.1 Reactor Operation and Decomposition Evaluation

A total of twenty decomposition runs were made in the course of this program. Performance for one run, 344-547, surpassed deposition rate and power consumption goals although a low conversion efficiency resulted. Results of run 344-547 compared to goal are:

	344-547	Goal
Deposition Rate	2.28 gm/hr-cm	2.0
Power Consumption	59 kWh/kg	60
Conversion Efficiency	17.1%	40

A significant amount of process characterization was obtained while meeting the expressed goals. Information was gathered concerning activation energy, effect of nozzle velocity, comparisons to the Model 8D reactor, as well as a better understanding of wall deposition in the cooled-wall reactor.

Table 3.2.1.a summarizes run conditions and results. Runs listed from 344-499 to 344-517 utilized conditions from the Model 8D experimentation[1]. The purpose of these runs was to check out equipment and determine if there were any fundamental differences in reactor performance when the only parameter changed was wall temperature. The Model 8D reactor operated with an inside wall temperature estimated at greater than 750°C. The cooled-wall reactor was operated to maintain the inner jar wall at 300°C. Silicon deposited vs. silicon fed data for the advanced reactor is compared with that of the Model 8D reactor in Figures 3.2.1a, b, c, and d. No difference is prevalent beyond that of experimental scatter.

Confirmation that the Model 8D and advanced reactors perform the same at the same feed conditions, while not unanticipated, was an important verification. This fact suggested that attainment of high deposition rates and low power consumption goals must be accomplished by the use of new conditions of feed rate, DCS concentration and rod temperature.

The remaining runs of the program provided a screening of the more aggressive conditions.

A larger feed nozzle was installed in the reactor in anticipation of high flow rates of feed. This forethought ultimately complicated data interpretation. The larger feed nozzle results in lower nozzle velocity. Nozzle velocity has a pronounced effect on conversion efficiency. Figure 3.2.1.e shows the relationship of conversion efficiency vs. nozzle velocity. Feed was 4.47 gm/hr-cm at 6 mole percent DCS and a single temperature for all points shown in Figure 3.2.1e. Table 3.2.1b provides deposition rate and conversion efficiencies that are adjusted upward by 30%, the result expected if runs were made at 850 ft/sec nozzle velocity. Run time and power consumption are lowered by 30%. The adjusted time is calculated from the equation:

$$wt. = (\text{feed rate})\ (\text{conversion}_1)\ (\text{time}_1)$$

where wt. and feed rate are equal.

$$(\text{conversion}_1)\ (\text{time}_1) = (\text{conversion}_2)(\text{time}_2)$$

Power consumption is the integral of instantaneous power vs. time. The shorter time has a direct impact on power consmption.

Inspection of Table 3.2.1b shows that one run, 344-547, demonstrated performance that exceeded goals for deposition rate and power consumption. Deposition rate was 2.28 gm/hr cm with power consumption of 59 kWh/kg. Conversion, moles of silicon deposited per mole of silicon fed, was only 17.1% as compared to a goal of 40%. Another run, 344-528, when adjusted for nozzle velocity effects, had performance that exceeded that of 344-547. Deposition rate was 2.38 gm/hr cm, power was 60 kWh/kg, and conversion was 32.1%. The improved deposition rate and conversion efficiency is attributed to larger final diameter rod and longer residence time.

Run 344-540 came very close to meeting conversion and power goals, adjusted, with values of 38.6% and 65

kWh/kg, respectively. The deposition rate, adjusted, was an impressive 2.87 gm/hr cm. This run had all the same conditions as run 344-528 except for rod temperature and final rod diameter. The higher rod temperature and larger diameter would tend to increase all performance parameters; a benefit for deposition rate and conversion but a detriment in power consumption.

Run 344-538 had a remarkably high, adjusted conversion of 46.1%. The high conversion is the result of high rod temperature. The high rod temperature also resulted in high power consumption, 80 kWh/kg, and lower final diameter due to power limitations. High rod temperature is considered unacceptable for routine operation.

All performance parameters appear feasible with conditions (except nozzle velocity) similar to run 344-528 or 344-540. Results (adjusted) and conditions for those runs are:

Run	344-528	344-540	Goal
Deposition Rate, gm/hr-cm	2.38	2.87	2.0
Power Consumption, kWh/kg	60	65	60
Conversion, %	32.1	38.6	40
Moles % DCS	10	10	
Final Diameter, mm	63	75	
Si Fed, gm/hr-cm	7.44	7.44	

Additional experimentation would be required to precisely establish desired run conditions. Additionally, optimization must address an entire plant design, not just reactor performance. Performance of 344-540, while using only 8.3% more power than the goal, resulted in 43.5% higher deposition rate and only 3.5% loss of conversion. The high deposition rate would reduce the number of reactors required to obtain a given capacity. The reduction of capital expenditure may be found to out-weigh the increase in operating cost if full economic evaluation were undertaken.

Additional observations were made during the course of this experimental program. Those observations were activation energy, jar deposition quantification, and mass balance information. Each area will now be discussed.

Activation energy was determined. Results are shown in Figure 3.2.1.f where molar conversion at 50 mm rod diameter vs. 1/T is plotted for the temperature range from 1273°K to 1423°K. The activation energy of 10 K cal/mole was calculated from the slope of the line in Figure 3.2.1.f and the Arrhenius equation. The 10 K cal/mole activation energy is typical of diffusion controlled silicon deposition processes.[2,3]

Deposition of silicon on the jar wall occurred in nearly all situations. The silicon deposition was predominantly a fine amorphous material. The powdery nature of the wall deposition caused operating inconvenience and some loss of silicon, but otherwise caused no problems.

Table 3.2.1c provides results of wall deposition for all runs on which information was obtained. The deposition ratio is expressed in kg silicon deposited on the jar wall per kg silicon deposited on the rods. Attempts were made to correlate jar deposition ratio to conversion, total silicon fed, rod temperature, and DCS feed rate. No correlation is apparent.

One run resulted in a polycrystalline silicon deposition layer forming over the amorphous layer on the jar wall. Calculation of heat transfer through the advanced reactor walls was done in an effort to understand this phenomenon. Three basic equations were used to make computations.

First, radiant energy transfer from the rods to the jar (the primary mechanism of heat transfer) can be expressed as:

$$Q_{total}/A_{rods} = (0.173)(\varepsilon_{Si})\left(\left(\frac{T_{Rods}}{100}\right)^4 - \left(\frac{T_{Jar}}{100}\right)^4\right)$$

Where:

Q total = BTU/hr of radiant energy transfer

A rods = Area of rods, ft^2

εSi = Emissivity of silicon = 0.7

T_{Rods} = ^{o}R of rods

T_{jar} = ^{o}R of jar

This correlation treats the jar as a black body. Experience has shown that treating the jar as a black body is sufficiently accurate for this engineering assessment.

The next equation is for energy transfer to the cooling fluid.

$$Q_{Total} = U\ A_{jar}\ \Delta T$$

Where:

Q_{Total} = BTU/Hr of Energy Transfer

U = BTU/ft^2 Hr^{o}F Overall Transfer Coefficient

A_{Jar} = Ft^2 Jar Area

ΔT = ^{o}F Temperature Difference

Finally, the overall transfer coefficient can be calculated by the following expression.

$$\frac{1}{U} = \frac{1}{U_{clean}} + \frac{1}{U_{fouling}}$$

U_{clean} was assumed to be infinite for a perfectly clean jar. With that assumption, ΔT became the temperature difference across the amorphous layer (fouling). $U_{fouling}$ was calculated by assuming the exposed jar coating, T_{jar}, is 750^{o}C; the temperature where DCS deposits polycrystalline silicon.

With the above equations and assumptions (T_{jar} = 750^{o}C, ΔT = 450^{o}C) for 50 mm diameter rods, $U_{fouling}$ was calculated to be 10.96 BTU/ft^2 hr^{o}F.

For run 344-528 the amorphous layer was 0.05

inch thick. Conversion of $U_{fouling}$ to thermal conductivity yielded:

$$K_{fouling} = 0.046 \text{ BTU/ft hr}^{\circ}\text{F}$$

This thermal conductivity is the order of magnitude expected for fine powders. The polycrystalline silicon deposition layer should be expected if the amorphous layer is formed with heat flux sufficient to raise the temperature to 750°C. The insulating nature of the amorphous layer allows the exposed surface temperature to increase to temperatures sufficient for polycrystalline silicon deposition.

While the wall deposition causes operating inconvenience, it also reduces instantaneous power consumption. Figure 3.2.1g shows instantaneous power vs. rod diameter for three runs. The three runs are a cooled wall run (344-505) with low deposition, a cooled wall run (344-528) with high wall deposition, and a Model 8D hot wall run (324-421). The instantaneous power for run 344-505 with low wall deposition was 30% higher than the other runs.

Gas chromatographic (GC) analysis of feed and vent streams of the reactor were employed to permit mass balance of the reactor. Seven runs were used to provide GC results. GC results as moles of product per 100 moles DCS feed are tabulated in Table 3.2.1d while Table 3.2.1e provides the results as pounds of vent gas constituents per kilogram of silicon produced. The GC results are instantaneous values for the rod diameter specified in Table 3.2.1d. These instantaneous conversions, as expected, are higher than run average values of Table 3.2.1a.

Run 344-505 resulted in essentially the same material balance as the Model 8D reactor. Expected DCS consumption would be 18.4 lb/kg in a production system. Other runs resulted in higher DCS consumption. Full characterization and correlation of mass balance information was not done because of the limited number of runs. Runs evaluated had low nozzle velocities, variable rod temperature, feed rates, feed com-

position and rod diameters. The general conclusion that was drawn is that lower conversion to silicon increases DCS consumption. High concentrations of unreacted DCS in the vent would tend to increase the extent of reaction with HCl to form trichlorosilane. With all reactor conditions maintained to allow 40% conversion, DCS consumption of 18.4 lb/kg would be expected.

3.2.2 Zone Refining Analysis

All decomposition runs were analyzed by resistivity measurements on zone refined samples. The currently accepted zone refining method at HSC, for the complete analysis of electrically active impurities in semiconductor grade silicon, is the multi-pass vacuum float-zone analysis. This method utilizes the different segregation coefficients and evaporation rates of impurity elements during the zone refining process to calculate impurity concentrations from the resistivity of the various zoned sections.

Table 3.2.2 contains donor and boron results. The average concentrations for donor of 1.43 ppba and boron of 0.24 ppba are well within the requirements for photovoltaic applications. Runs 344-500, 344-501 and 344-537 have exceptionally high purity. Average boron content for these runs was 0.07 ppba while donor content was 0.41 ppba. These low impurity levels are indicative of the purity potential of the DCS decomposition process.

3.2.3 Mass Spectrographic Tests

Mass spectrographic analysis of several runs was used to determine trace metal impurity concentrations. The determination of trace metal impurities in semiconductor grade silicon, requires the use of a technique capable of sub-part per million analysis. HSC uses an MS 702 spark source mass spectrometer for the determination of trace metal impurities at parts per billion atomic (ppba) levels. Spark source mass spectrometry differs from conventional mass spectrometry in that

the spark source generates ionized atoms rather than molecular species. Thus, the spark source instrument is an elemental analysis instrument. The resultant mass spectra are recorded on a photographic plate. Semi-quantitative analysis is accomplished by making a graded exposure on the plate. This instrument has a detection range of 3-10 ppba for most elements, but as high as 50-100 ppba for the elements Ni, Fe and Co. HSC performs mass spectrographic tests on the freeze-out section of a 1-pass zone refined sample. The impurities are concentrated in the freeze-out section.

Results of the analysis for trace metal impurities in silicon produced in the advanced reactor show impurity levels far better than required for photovoltaic applications. Three samples analyzed in the spark source mass spectrometer yielded values for nineteen elements that are significantly less than the minimum levels necessary for high-efficiency photovoltaic cell applications. The impurity levels are quantified by assigning a range from minimum to maximum of impurity concentration in the sample.

Table 3.2.3 gives the average minimum and maximum values for the three samples analyzed. Care must be exercised in use of the values due to the semi-quantitative nature of the freeze-out analysis method. Also shown is the range, the lowest minimum and the highest maximum for samples. Minimum average values of zero were recorded for elements that were not detected in any of the samples. Therefore, their corresponding maximum values are the detection limits for those particular elements, i.e. undetected elements could be present but are at least below the detection limit, which is stated as the maximum level.

3.2.4 Fourier Transform Infrared Tests

Carbon content in the polycrystalline silicon was determined by Fourier Transform Infrared Absorption Measurements. Results are included with donor and boron results in Table 3.2.2. Most of the samples contained 0.1 ppma carbon,

essentially the detection limit of this test method. The highest carbon content was 0.37 ppma. The average carbon content was 0.15 ppma, which is well within the purity requirements for photovoltaic applications.

3.3 Materials of Construction Testing

Standard Siemen's reactors are constructed of high-purity materials. Typically, the electrodes and baseplates are made from specially purified metals. The bell jars are high-purity quartz. It is reported that quartz bell jars can be eliminated by use of a silver-lined metal bell jar.[4] As photovoltaic applications have less stringent purity requirements than those of the electronics industry, it is desirable to identify materials of construction that will meet photovoltaic requirements at a lower cost.

Five commonly available materials were selected for evaluation. The materials screened were 304 Stainless Steel, 316 Stainless Steel, Monel 400, Carbon Steel 1010-1020 and Hastalloy B.

To screen materials of construction, a simple test was devised. A length of tubing was inserted directly into an experimental-scale decomposition reactor. A set of 3 runs was made for each material. Baseline and burnout runs were performed between each set of 3 runs. Boron and donor concentrations were determined by zone refining analysis. Metallic impurities were measured with a spark source mass spectrometer. Carbon content was measured by infrared absorption. The potential materials of construction were ranked according to their impact on purity of the silicon grown in the decomposition reactor.

Figure 3.3 represents the experimental-scale Siemen's reactor with the tubing sample installed. The tubing was 1/4 inch OD. The length was selected so that the ratio of surface area to total weight of silicon produced was the same as the ratio of jar surface area to total silicon produced in a production-scale reactor. The tubing was cleaned with solvent

prior to insertion in the reactor.

When the reactor set-up was completed, silicon was produced in a conventional manner. Trichlorosilane and hydrogen were fed to the reactor. TCS was used because of its availability at this reactor, the abundance of base data, and the advantage of a slower deposition rate allowing longer run times in which impurities could be incorporated in the silicon. Hydrogen flowing through the tubing was the coolant. The temperature of the hydrogen exiting the tubing was maintained at 300°C.

A sample from each run was subjected to zone refining analysis, described in Section 3.2.2. The sample was an entire silicon rod to assure results representative of a full run. Metallic impurities were determined on one or more runs for each material using mass spectrometer analysis as described in Section 3.2.3. A sample from a run of each material was subjected to infrared absorption analysis for carbon determination. The sample for this measurement was cut from the polycrystalline rod parallel to and approximately 1 mm from the slim rod.

Table 3.3.a provides results for boron, donor, aluminum or arsenic, and carbon for the materials of construction tests. No material caused significant contribution of electrically active impurities. All materials had significant carbon contribution.

Only the first test run for each material produced silicon that was typical of semiconductor-grade silicon with respect to zoning properties. Crystals grown from subsequent runs would not remain single. The high carbon content is presumed responsible for loss of singularity. This is further supported by the evaluation of a second phase that migrates to the surface of the molten zone during zone refining. X-ray diffraction found the second phase to be silicon carbide.

Table 3.3.b provides mass spectrographic results. No material resulted in gross metallic contamination of the silicon. Table 3.3.c provides nominal composition of the materials tested. An inference can be made as to the amount of corrosion

experienced by the tubing by comparing the metallic impurities found in the silicon with the composition of the materials.

Rated from 1=best to 5=worst, the following rank order was established for electrically active and carbon contributions and corrosion.

Material	Electrically Active	Carbon	Corrosion
304 S.S.	3	3	2
Monel 400	5	1	5
Carbon Steel	4	4	3
Hastalloy B	2	5	1
316 S.S.	1	2	4

No material need be excluded from consideration for use in a decomposition reactor based on the materials of construction scans. Additional and more detailed evaluation is required to determine if carbon contribution can be reduced. Low-carbon-content alloys of the listed materials may be sufficient to overcome carbon contribution. Corrosion should be evaluated on a long-term test intended to determine service life of equipment as well as contribution of metallic impurities to the silicon produced.

3.4 Reflectivity vs. Power Tests

The impact of reflectivity on power consumption was to be investigated experimentally. A theoretical evaluation was performed in place of experimentation because of the amorphous deposition on the bell jar wall, a condition that makes control of reflectivity impossible.

The primary mode of energy transfer from a silicon rod to the jar wall is by radiant heat transfer. Kern[5] expresses radiant heat transfer between concentric cylinders by:

$$Q = \frac{A_1\sigma}{1/\varepsilon_1 + (r_1/r_2)\ (1/\varepsilon_2 - 1)} \quad (T_1^4 - T_2^4)$$

Where: Q = Total energy transferred, BTU/Hr.
σ = Stefan-Boltzmann constant, 0.173×10^{-8} BTU/Hr $ft^2(^oR)^4$
A_1 = Area of the hot surface, ft^2.
ε_1 = Emissivity of hot surface = 0.7 for silicon.
ε_2 = Emissivity of cold surface.
r_1 = Radius of inner cylinder.
r_2 = Radius of outer surface.
T_1 = Temperature of hot surface, ^oR.
T_2 = Temperature of cold surface, ^oR.

This equation can be used to determine the impact of jar emissivity on radiant energy loss from a silicon rod to the jar. Rearranging the equation provides heat flux from the silicon rod.

$$Q/A = \frac{\sigma}{1/\varepsilon_1 + (r_1/r_2)\ (1/\varepsilon_2 - 1)} \quad (T_1^4 - T_2^4)$$

If T_1 and T_2 are kept constant

$$Q/A = \frac{K}{1/\varepsilon_1 + (r_1/r_2)\ (1/\varepsilon_2 - 1)}$$

Where: $K = \sigma(T_1^4 - T_2^4)$

A conventional decomposition reactor design would have an initial r_1/r_2 of approximately 1/100. The final r_1/r_2 would be approximately 1/8.

Table 3.4 shows heat flux vs. bell jar emissivity for typical initial and final rod diameters. For r_1/r_2 = 1/100, the initial condition, an 0.1 emissivity reduces the heat flux by only 6% as compared to a black body. For r_1/r_2 = 1/8 the heat flux is reduced by 44%.

In a production process it is necessary to traverse the entire range of r_1/r_2. Calculation of run average heat flux for ε_2 = 0.1 and ε_2 = 0.3 found heat flux to be 0.506K and 0.633K, where $K = \sigma(T_1^4 - T_2^4))$ respectively. These heat flux values represent a 27.7% and 9.6% reduction of run average heat flux as compared to the case where ε_2 is 1.0.

If elimination of amorphous silicon coating on the bell jar could be attained, it would be worthwhile to further pursue a bell jar with an emissivity of 0.1. The 27.7% reduction in heat flux would reduce power consumption by approximately 16 kWh/kg, to 44 kWh/kg.

3.5 PDU Operation and Evaluation

The DCS PDU constructed during the preceeding phases operated extremely well during this project phase. DCS was produced at will in both quantity and quality desired. No characterization or optimization was undertaken or required beyond that reported previously.[1]

4.0 Conclusions

The advanced reactor with its cooled walls allows higher DCS feed rates and concentrations to the decomposition reactor. The higher DCS rate allows the production of silicon at greater than 2.0 gm/hr-cm and with power consumption of 60 kWh/kg.

This effort confirms that the performance objectives established for a silicon production facility based on the chemical vapor decomposition of dichlorosilane are reasonable and attainable. Those performance objectives were used in the economic evaluation of a 1000 MT/yr plant where cost of product, without profit, was determined to be $15.60/kg.[1]

5.0 New Technology

No new technology has been identified in the course of this contract.

6.0 References

1. Hemlock Semiconductor Corporation, Final Report, "Development of a Polysilicon Process Based on Chemical Vapor Deposition (Phase 1 and Phase 2)", JPL Contract 955533, August, 1982.

2. Bean, K. E., "Chemical Vapor Decomposition Applications in Microelectronics Processing", Thin Solid Films, 83:1173 (1981).

3. Bloem, J. and L. J. Gilong, Current Topics in Materials Science, Vol. I, Amsterdam (1978).

4. United States Patent No. 4,179,530, issued to Franz Koppl, Dec. 18, 1979.

5. Kern, D. Q., "Process Heat Transfer", McGraw Hill Book Co., 1950.

Table 3.2.1a DCS Reactor Process Evaluation -- Reactor Performance Data

Run Number	Mole %	Run Time (Hrs)	Rod Diameter* (mm)	Si Fed (gh-1 cm-1)	Si Deposition (gh-1 cm-1)	Run Average Conversion (%)	Power Consumption (kWh/kg)
344-499	6	16.0	33-34	4.46	1.24	28.1	86
344-500	4	22.4	39-40	4.06	1.32	32.6	104
344-501	4	34.0	53-54	4.06	1.49	36.7	118
344-505	6	37.0	55-59	4.47	1.58	35.2	103
344-507	6	27.7	48-49	5.28	1.48	28.1	108
344-508	6	18.0	38-39	6.09	1.43	23.5	94
344-510**	6	23.1	47-49	6.09	1.78	29.2	96
344-516	5.5	21.3	41-42	4.47	1.39	34.0	102
344-517	6	28.7	54-56	6.09	1.88	30.9	95
344-528**	10	38.0	60-63	7.44	1.83	24.7	78
344-534	6	36.0	48-53	4.47	1.25	27.9	131
344-535	6	30.7	44-49	4.47	1.28	28.6	124
344-536	6	77.9	60-66	4.47	0.94	21.1	133
344-537	6	36.0	65-74	10.15	2.47	23.4	76
344-538	6	23.7	48-49	4.47	1.57	35.5	104
344-540	10	39.3	65-75	7.44	2.21	29.7	85
344-541	6	42.5	52-55	4.47	1.19	27.7	120
344-544**	6	30.0	46-48	4.47	1.30	29.2	107
344-545	6	39.5	64-66	4.47	1.81	40.6	107
344-547	9	17.0	43-45	13.39	2.28	17.1	59

* Range of final rod diameter measurements.
** Reactors experienced operating problems.

Table 3.2.1b DCS Reactor Process Evaluation -- Reactor Performance Data

Run Number	Mole %	Run Time (Hrs)		Rod Diameter* (mm)	Si Fed (gh-1 cm-1)	Si Deposition (gh-1 cm-1)		Run Average Conversion (%)		Power Consumption (kWh/kg)	
344-499	6	16.0		33-34	4.46	1.24		28.1		86	
344-500	4	22.4		39-40	4.06	1.32		32.6		104	
344-501	4	34.0		53-54	4.06	1.49		36.7		118	
344-505	6	37.0		55-59	4.47	1.58		35.2		103	
344-507	6	27.7		48-49	5.28	1.48		28.1		108	
344-508	6	18.0		38-39	6.09	1.43		23.5		94	
344-510**	6	23.1		47-49	6.09	1.78		29.2		96	
344-516	5.5	21.3	▼	41-42	4.47	1.39	▼	34.0	▼	102	▼
344-517	6	28.7		54-56	6.09	1.88		30.9		95	
344-528**	10	38.0	29.2	60-63	7.44	1.83	2.38	24.7	32.1	78	60
344-534	6	36.0	27.7	48-53	4.47	1.25	1.62	27.9	36.3	131	101
344-535	6	30.7	23.6	44-49	4.47	1.28	1.66	28.6	37.2	124	95
344-536	6	77.9	59.9	60-66	4.47	0.94	1.22	21.1	27.4	133	102
344-537	6	36.0	32.4	65-74	10.15	2.47	2.76	23.4	26.1	76	68
344-538	6	23.7	18.2	48-49	4.47	1.57	2.04	35.5	46.1	104	80
344-540	10	39.3	30.2	65-75	7.44	2 21	2.87	29.7	38.6	85	65
344-541	6	42.5	32.7	52-55	4.47	1.19	1.55	27.7	36.0	120	92
344-544**	6	30.0		46-48	4.47	1.30		29.2		107	
344-545	6	39.5		64-66	4.47	1.81		40.6		107	
344-547	9	17.0		43-45	13.39	2.28		17.1		59	

* Range of final rod diameter measurements.
**Reactors experienced operating problems.

▼Values are adjusted for nozzle velocity effect. This is the result expected had 850 ft/sec nozzle velocity been used.

Table 3.2.1c

Jar Wall Deposition

Run Number	Kg Si on Jar per Kg Silicon Deposited
344-499	*
344-500	0.003
344-501	*
344-505	0.0008
344-507	*
344-508	*
344-510	0.005
344-516	*
344-517	*
344-528	0.014
344-534	≈0
344-535	≈0
344-536	0.033
344-537	0.023
344-538	≈0
344-540	0.021
344-541	*
344-544	0.0019
344-545	0.00071
344-547	0.020

* Not Determined

Table 3.2.1d

Gas Chromatographic Results

Run	Approx. Dia.	Products* Si	HCl	Moles/100 Moles Si Fed DCS	TCS	STC
344-505	54	37.2	18.7	12.9	38.1	10.5
344-536	27	23.0	7.2	44.2	29.5	3.3
344-537	70	31.2	3.4	21.9	37.8	9.9
344-538	48	31.8	2.7	18.8	38.1	10.7
344-540	70	33.6	1.8	16.3	37.6	12.4
344-541	54	30.1	2.4	24.5	36.0	9.4
344-547	46.5	32.2	7.2	21.6	38.0	8.1
Model 8D	54	37.5	7.3	11.3	35.3	14.8

* Instantaneous

Table 3.2.1e

Gas Chromatographic Results

Run 344-	Conversion*	Vent Gases (lb/kg of Si produced) HCl	DCS	TCS	STC	DCS (lb/kg Si) Fed	Consumed
505	37.2	1.44	2.72	10.90	3.77	21.1	18.4
536	23	0.90	15.10	13.65	1.92	34.16	19.06
537	31.2	0.31	5.51	12.90	4.24	25.18	19.67
538	31.8	0.24	4.64	12.75	4.49	24.71	20.07
540	33.6	0.15	3.81	11.91	4.93	23.39	19.57
541	30.1	0.23	6.39	12.73	4.17	26.10	19.71
547	32.2	0.64	5.27	12.56	3.36	24.40	19.13
Model 8D	37.5	0.56	2.36	10.08	5.27	20.95	18.59

* Instantaneous, see Table 3.2.1d on page 21.

Table 3.2.2

Reactor 344, Purity Results for DCS Feed

Run #	Donor ppba	Boron ppba	Carbon ppma
499	2.03	1.38	0.1
500	0.46	0.05	0.1
501	0.50	0.07	0.1
505	2.1	0.09	0.22
507	0.98	0.07	0.1
508	2.3	0.08	0.1
510	2.7	0.06	0.37
516	4.3	0.08	0.1
517	1.3	0.10	---
528	3.66	0.37	0.1
534	2.28	0.17	0.22
535	0.85	0.14	0.18
536	0.82	0.24	---
537	0.27	0.09	0.1
538	1.1	0.37	0.32
540	0.22	0.46	0.1
541	0.3	0.11	0.1
544	1.3	0.25	---
545	0.3	0.41	0.1
547	0.8	0.17	0.1
Average	1.43	0.24	0.15

Table 3.2.3

Mass Spectrographic Analysis

of Three Polycrystalline Silicon Samples

(Concentrations in Parts Per Billion Atomic)

Element	Averages		Range	
	Minimum	Maximum	Minimum	Maximum
Al	3.6	11	0	23
Fe	2.0	6.9	0	9
Ni*	0	2.1		
Na	1.6	5.6	0.4	15
Mg	0.6	2.0	0	5.6
Co*	0	0.2		
Ti	0.1	0.4	0	0.6
V	0.1	0.5	0	1.3
Cr	0.9	2.8	0.5	5.3
Mn	0.1	0.2	0	0.3
Cu	0.3	1.0	0.2	2.0
Zn*		0.3		
Zr*	0	0.8		
Nb*	0	0.1		
Mo*	0	0.6		
Pd*	0	0.5		
Ag*	0	0.3		
Sn*	0	0.4		
W*	0	0.4		

* Undetected. Value shown is detection limit.

Table 3.3.a

Material of Construction Testing Results for Electrically Active Impurities and Carbon

Material		Reactor Run No.	Boron ppba	Donor ppba	Al (+) As (-)	carbon ppma
Baseline/BO		394-184	0.11	1.53	0.01	
304 SS		394-185	0.05	1.77	0.03	
304 SS	(1)	394-186	0.07	0.57	0.20	7.36
304 SS	(1)	394-187	0.07	0.84	0.15	
Baseline/BO		394-188	0.11	0.87	0.12	
Monel #1		394-189	0.13	1.05	0.17	4.56
Monel #2 (1)		394-190	0.29	1.08	0.49	3.22
Monel #3 (1)		394-191	0.04	0.45	0.12	
Baseline		394-192	0.07	0.51	0.00	
Carbon Steel #1		394-193	0.07	0.48	0.04	1.49
Carbon Steel #2	(1)	394-194	0.07	0.98	0.16	8.59
Carbon Steel #3	(1)	394-195	0.04	1.14	-.08	
BO		394-196	0.03	0.45	0.10	
Hastalloy #1		394-198	0.10	1.04	0.10	0.14
Hastalloy #2	(1)	394-199	0.05	0.43	0.00	9.86
Hastalloy #3	(1)	394-200	0.08	0.55	0.06	
Baseline		394-201	0.04	0.49	0.00	
Baseline		394-202	0.08	0.30	0.03	9.34
316 SS #1		394-203	0.05	1.28	0.41	
316 SS #2	(1)	394-204	0.04	0.33	0.03	5.77
316 SS #3	(1)	394-205	0.03	0.39	0.01	

(1) Lost singularity.

Table 3.3.b

Mass Spectrographic Analysis

of Polycrystalline Silicon

(Concentrations in Parts Per Billion Atomic)

Element	394-185 304-SS #1	394-186 304-SS #2	394-189 Monel #1	394-190 Monel #2	394-193 Carbon Steel #1	394-194 Carbon Steel #2	394-199 Hastalloy B #2	394-204 316 SS #2	394-192 Baseline
Al	6.0	60	190	57	207	20	18	63	20
Fe	2.9	2.9	81	27	31	31	2.6	93	3
Ni	2.0	1.9	1.8	1.8	2.0	20	1.7	2.0	2
Na	3.9	3.9	3.6	1.4	0.3	0.3	1.0	4.2	1.4
Mg	0.6	5.1	16	4.8	0.6	0.6	1.2	5.4	1.7
Co*	1.3	1.3	1.2	1.2	1.3	1.3	1.2	1.4	1.2
Ti	0.2	18	17	51	5.4	18	1.5	20	17
V	0.1	0.1	0.3	0.3	0.1	0.1	0.1	0.1	0.1
Cr	4.5	1.7	15	15	0.3	0.3	0.3	17	45
Mn	0.1	0.1	0.1	0.1	0.1	0.1	0.3	0.1	0.1
Cu	19	6.0	54	18	19.5	20	5.1	63	54
Zn*	0.2	0.2	0.2	0.2	0.3	0.3	0.3	0.3	0.3
Zr	0.8	0.8	2.1	0.7	0.8	0.8	0.7	0.8	0.7
Nb*	0.1	0.1	0.1	0.1	0.1	0.1	0.1	0.1	0.1
Mo	0.5	5.4	5.1	15	0.5	54	5.1	6.1	5.1
Pd*	0.5	0.5	0.4	0.4	0.5	0.5	0.4	0.5	0.5
Ag*	0.2	0.2	0.2	0.2	0.2	0.2	0.2	0.3	0.2
Sn*	0.4	0.4	0.4	0.4	0.4	0.4	0.3	0.4	0.4
W*	0.4	0.4	0.4	0.4	0.4	0.4	0.4	0.5	0.4

* Non-detectable, value is detection limit.

Table 3.3.c

Materials of Construction Testing

Nominal Compositions of the Materials, in Wt. %

	304 SS	Monel 400	Carbon Steel	Hastalloy B	316 SS
Fe	65+	1.25	95+	2	60+
Ni	8-10	66.5		65.4	10-14
Mg	<2				<2
Co				2.5	
Cr	18-20			1.0	
Mn	<0.3	1.0	1.65	1.0	<0.3
Cu		31.5	tr.		
Mo				28.0	2-3

Table 3.4

Heat Flux vs. Jar Emissivity

Jar Emissivity	Heat Flux Q/A for r_1/r_2 = 1/100	Heat Flux Q/A for r_1/r_2 = 1/8	% Flux Reduction vs. that where $\varepsilon_2 = 1.0$ for r_1/r_2 = 1/100	% Flux Reduction vs. that where $\varepsilon_2 = 1.0$ for r_1/r_2 = 1/8
$E_2 = 1.0$	0.7K	0.7K	0	0
0.9	0.699K	0.693K	0.1	1.0
0.8	0.698K	0.685K	0.3	2.1
0.7	0.698K	0.675K	0.3	3.5
0.6	0.697K	0.661K	0.4	5.6
0.5	0.695K	0.644K	0.7	8.0
0.4	0.693K	0.619K	1.0	11.6
0.3	0.689K	0.581K	1.5	17.0
0.2	0.681K	0.518K	2.7	26.0
0.1	0.658K	0.392K	6.0	44.0

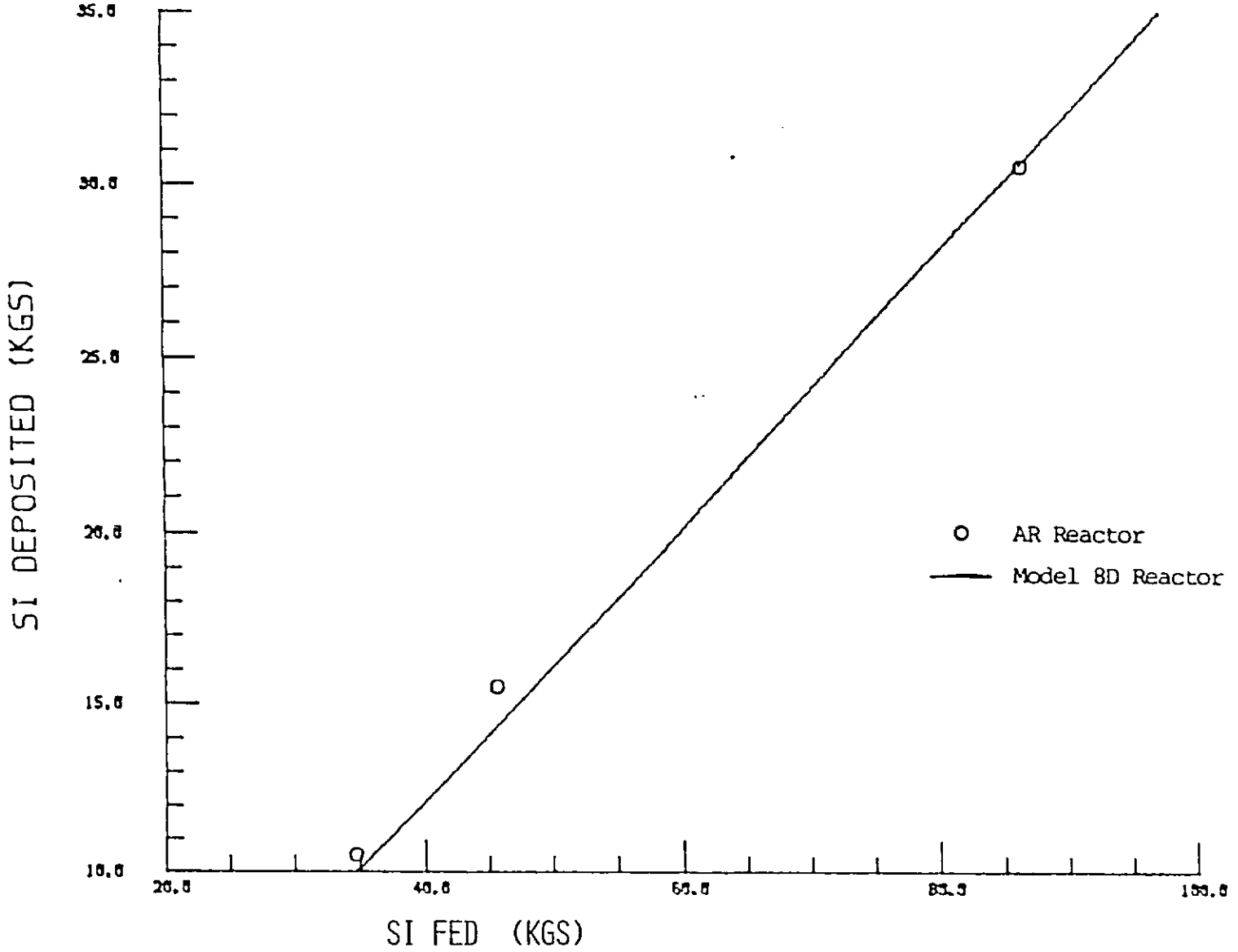

Figure 3.2.1a

CONVERSION DATA PLOT (6% DCS 4.46 GM/HR/CM FEED)

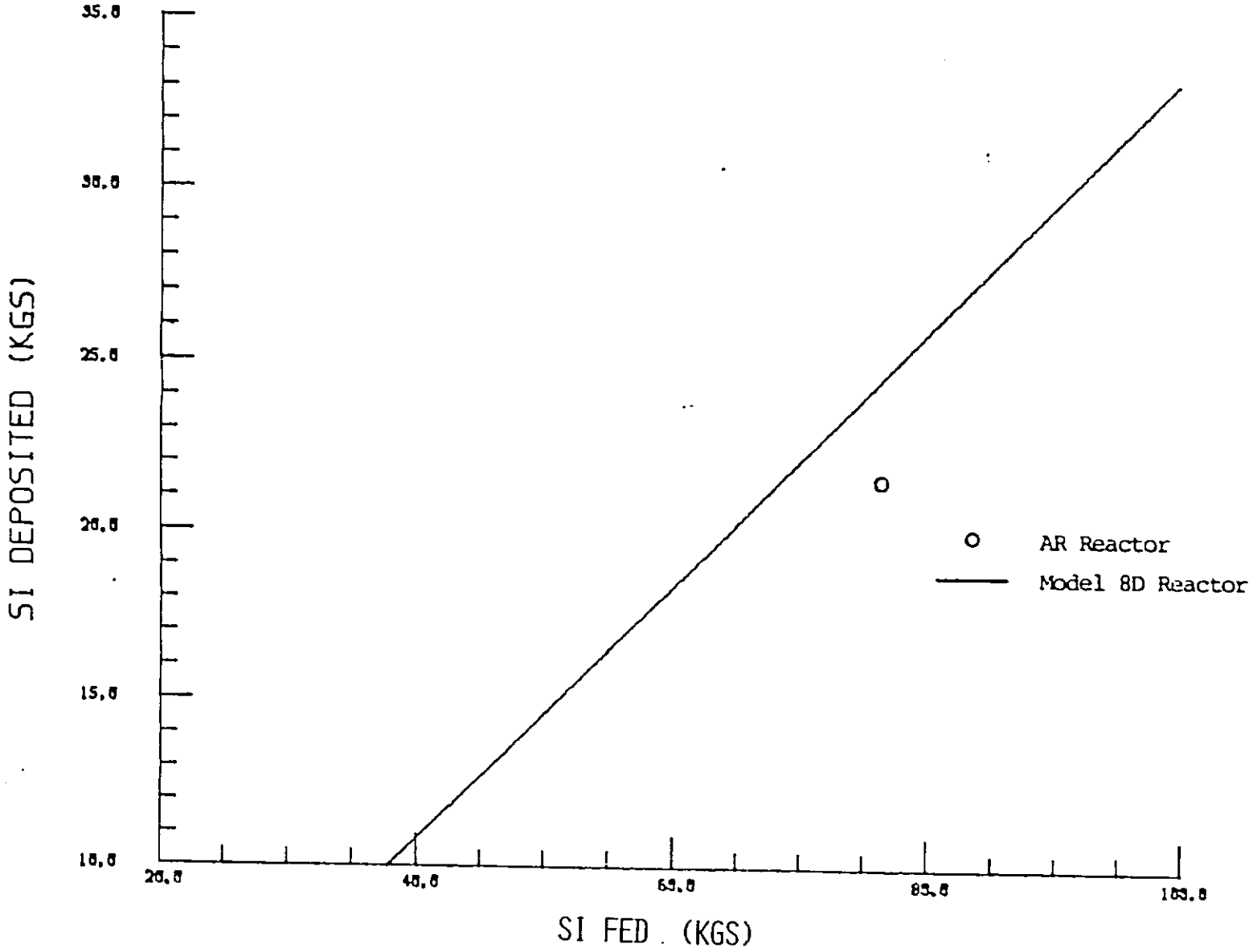

Figure 3.2.1b

CONVERSION DATA PLOT (6% DCS 5.20 GM/HR/CM FEED)

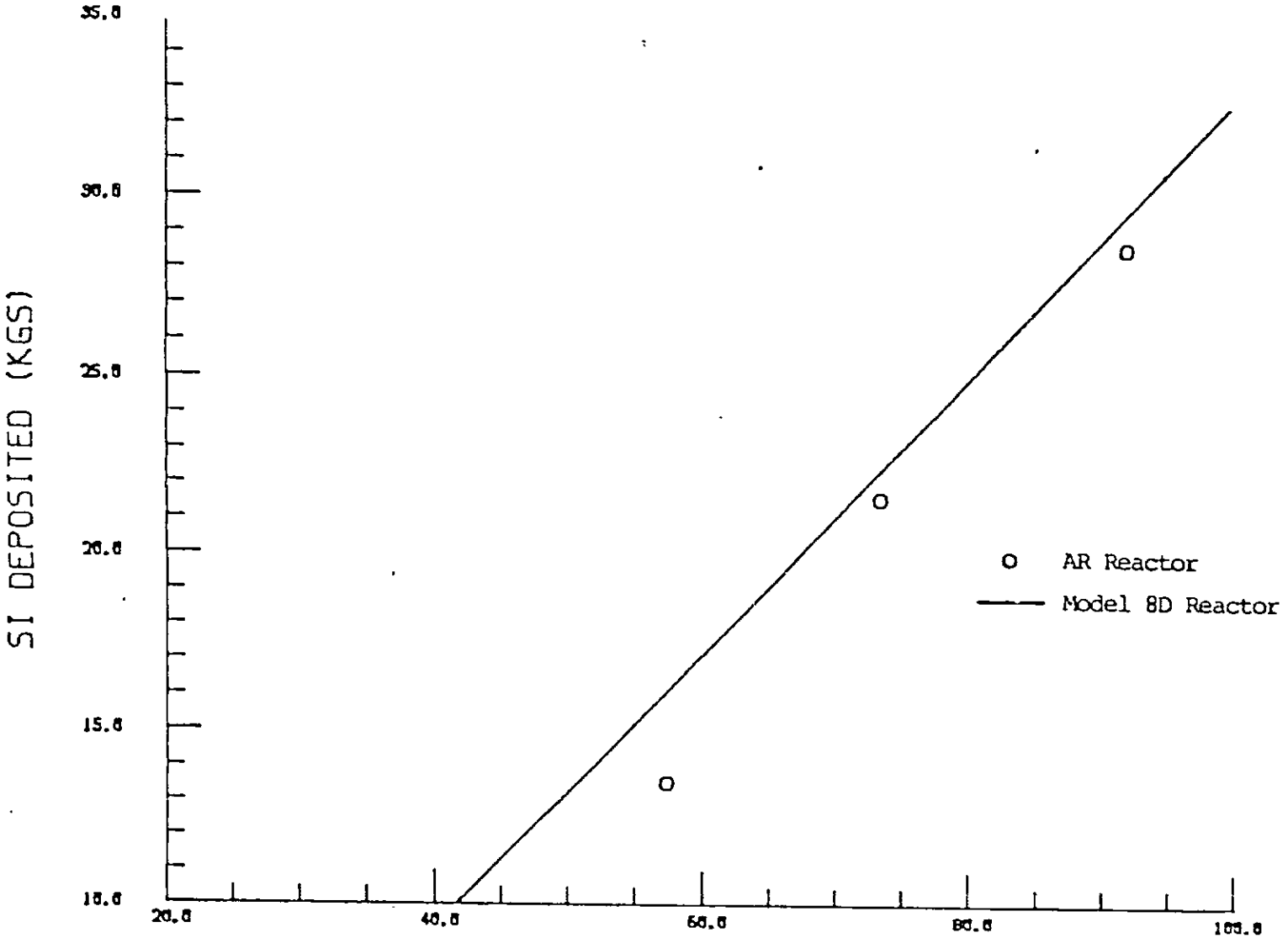

Figure 3.2.1c

CONVERSION DATA PLOT (6% DCS 6.09 GM/HR/CM FEED)

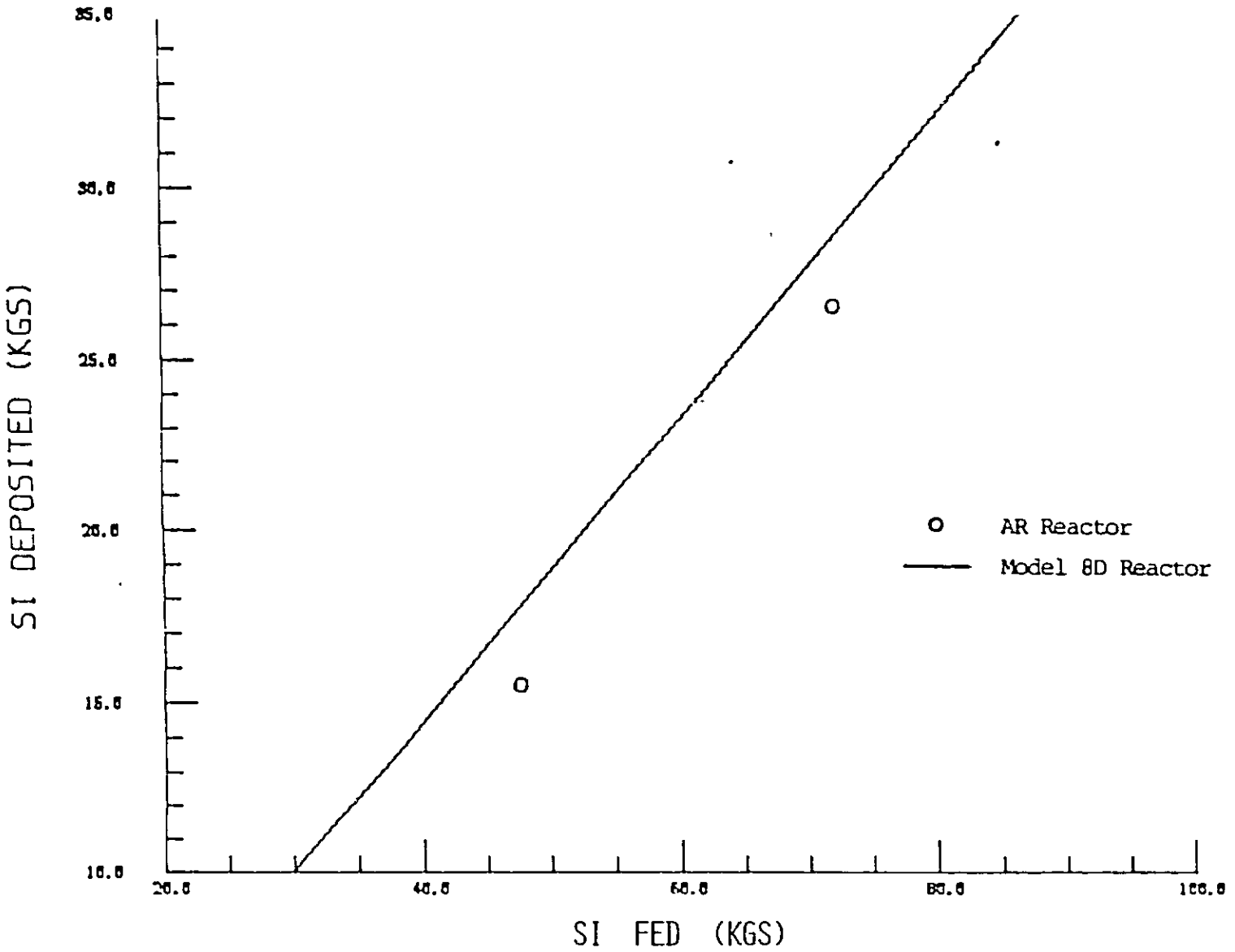

Figure 3.2.1d

CONVERSION DATA PLOT (4% DCS 4.06 GM/HR/CM FEEI)

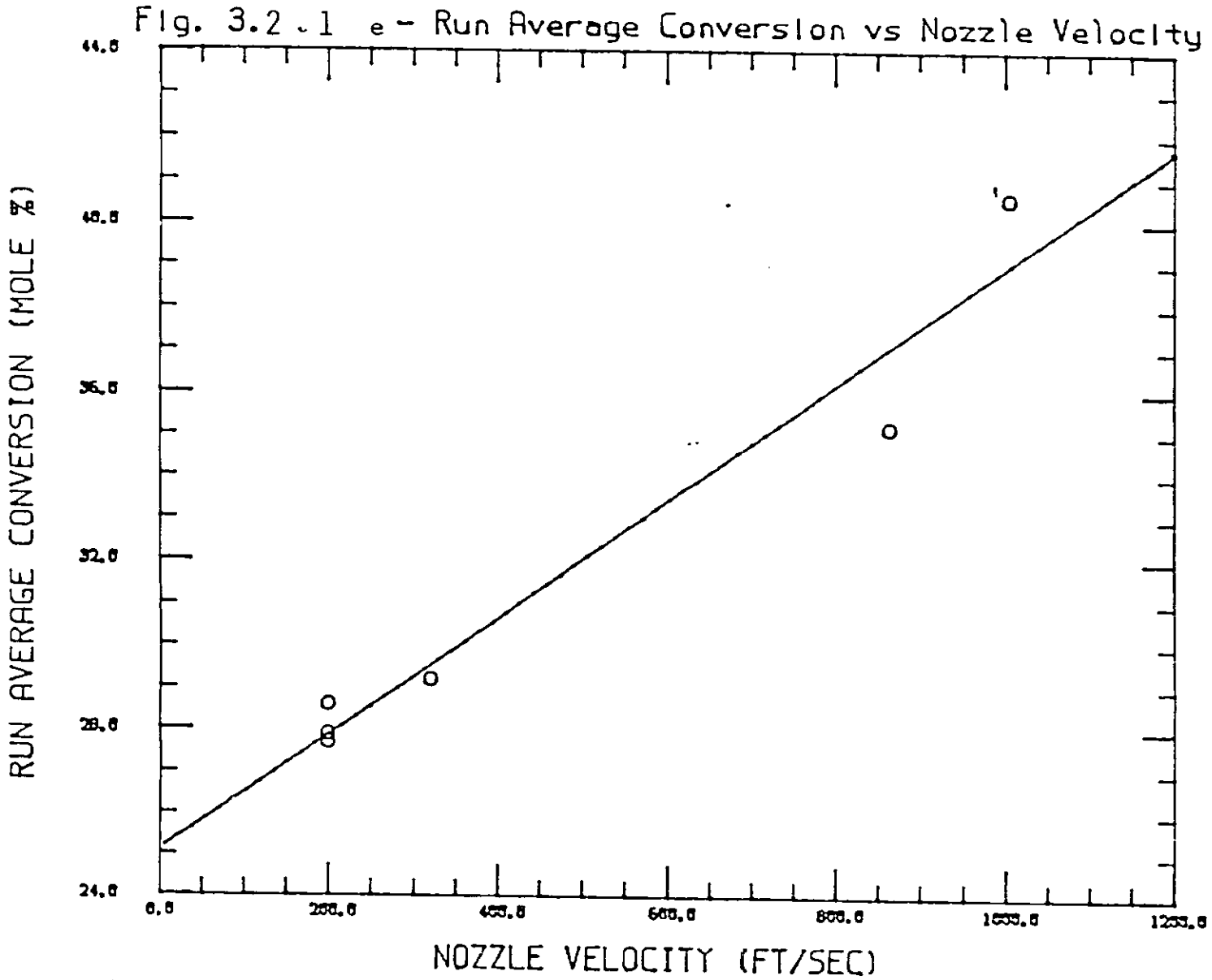
Fig. 3.2.1 e - Run Average Conversion vs Nozzle Velocity
RUN AVERAGE CONVERSION (MOLE %)
44.0
40.0
36.0
32.0
28.0
24.0
0.0
200.0
400.0
600.0
800.0
1000.0
1200.0
NOZZLE VELOCITY (FT/SEC)

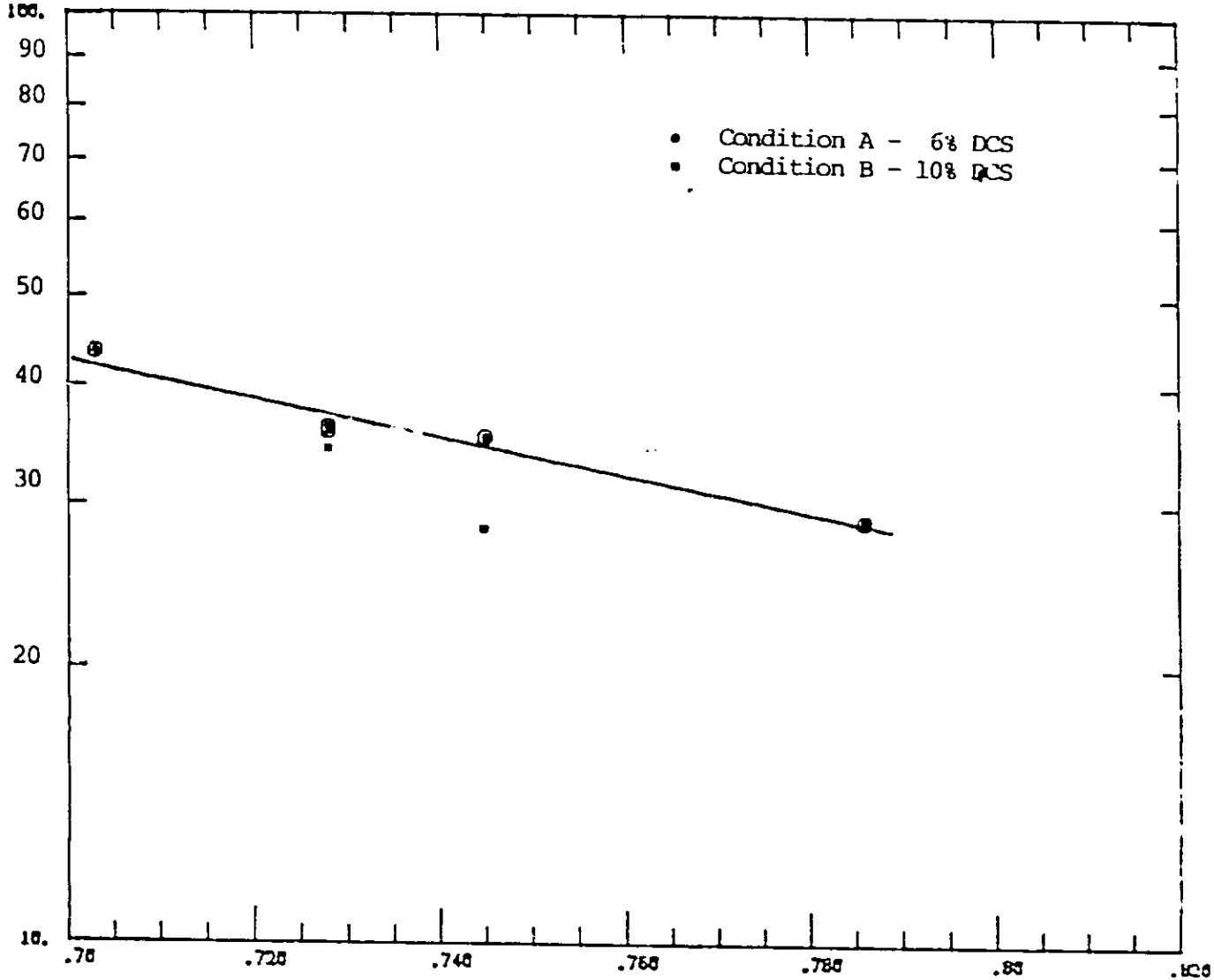

Figure 3.2.1f

CONVERSION EFFICIENCY vs $^1/_T$

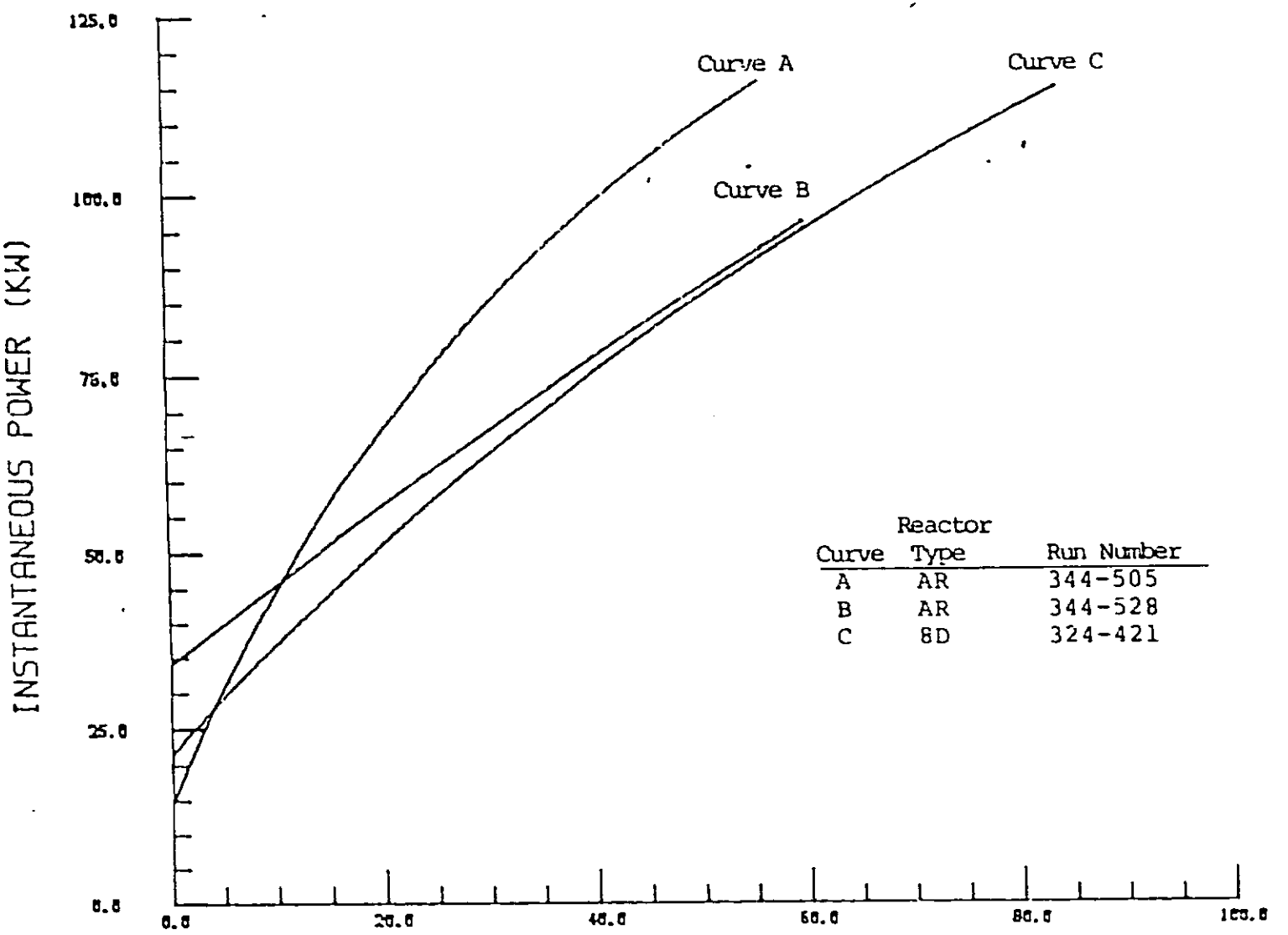

Curve	Reactor Type	Run Number
A	AR	344-505
B	AR	344-528
C	8D	324-421

Figure 3.2.1g

POWER vs DIAMETER DATA PLOT

FIGURE 3.3
MATERIALS OF CONSTRUCTION
REACTOR CONFIGURATION